http://www.kidney-international.org

Triptolide reduces proteinuria in experimental membranous nephropathy and protects against C5b-9-induced podocyte injury *in vitro*

Zhao-Hong Chen[1,2], Wei-Song Qin[1,2], Cai-Hong Zeng[1], Chun-Xia Zheng[1], Yi-Mei Hong[1], Yi-Zhou Lu[1], Lei-Shi Li[1] and Zhi-Hong Liu[1]

[1]*Research Institute of Nephrology, Jinling Hospital, Nanjing University School of Medicine, Nanjing, China*

Membranous nephropathy is a major cause of nephrotic syndrome in adults where podocyte injuries were found to mediate the development of proteinuria. Triptolide, a major active component of *Tripterygium wilfordii Hook F*, has potent immunosuppressive, anti-inflammatory and antiproteinuric effects. To study its antiproteinuric properties, we established an experimental rat model of passive Heymann nephritis and a C5b-9 injury model of podocytes *in vitro*. Treatment or pretreatment with triptolide markedly reduced established proteinuria as well as the titer of circulating rat anti-rabbit IgG antibodies in these nephritic rats, accompanied by a reduction in glomerular C5b-9 deposits. Expression of desmin, a marker of podocyte injury, diminished after triptolide treatment, whereas quantitative analysis of mean foot process width showed that effacement of foot processes was substantially reversed. In *in vitro* studies we found that triptolide deactivated NADPH oxidase, suppressed reactive oxygen species generation and p38 mitogen-activated protein kinase, and restored RhoA signaling activity. Triptolide did not interfere with the formation of C5b-9 on the membrane of podocytes. Thus, triptolide reduces established heavy proteinuria and podocyte injuries in rats with passive Heymann nephritis, and protects podocytes from C5b-9-mediated injury.

Kidney International (2010) **77,** 974–988; doi:10.1038/ki.2010.41; published online 10 March 2010

KEYWORDS: complement system; passive Heymann nephritis; podocyte; proteinuria; triptolide

Correspondence: *Zhi-Hong Liu, Research Institute of Nephrology, Jinling Hospital, Nanjing University School of Medicine, Nanjing 210002, China. E-mail: zhihong--liu@hotmail.com*

[2]These authors contributed equally to this work and are to be considered first authors.

Received 25 July 2009; revised 14 December 2009; accepted 13 January 2010; published online 10 March 2010

Immune-mediated podocyte injuries are crucial in the development of proteinuria in many kinds of glomerulonephritis, including membranous nephropathy. Membranous nephropathy is a major cause of nephrotic syndrome in adults. It accounts for 10% of primary glomerulonephritis in China and approximately 30% in Western countries.[1,2] It is characterized by subepithelial immune deposits, podocyte foot process effacement and expansion of the glomerular basement membrane (GBM).[3] Complement activation and C5b-9 formation triggered by immune complex have major roles in the development of tissue damage, whereas podocytes are important target cells during this process.[4,5] Although some patients with membranous nephropathy remit spontaneously, therapeutic strategies for those with persistent severe proteinuria and progressive loss of renal function are toxic and not uniformly effective. Approximately one-third of patients may develop progressive renal disease.[6]

Triptolide, an active component of the medicinal plant *Tripterygium wilfordii Hook F* (TWHF),[7] has potent immunosuppressive and anti-inflammatory therapeutic effects. Triptolide has been shown to inhibit the proliferation of lymphocytes and induces apoptosis of lymphocytes and dendritic cells.[8,9] Triptolide is also a potent inhibitor of NF-kappa B and NF AT-mediated transcription.[10] These characteristics of triptolide helped to partially explain the therapeutic effects of TWHF extracts in autoimmune diseases. In addition to the above properties, extracts of TWHF could alleviate glomerular albumin permeability induced by various stimuli such as protamine, tumor necrosis factor (TNF)-α and the serum from patients with focal segmental glomerular sclerosis *in vitro*,[11] which implicated an intriguing possibility that TWHF might protect the glomerular filtration barrier. Zheng *et al*,[12] reported that triptolide ameliorated puromycin aminonucleoside (PAN)-mediated podocyte injuries *in vivo* and *in vitro*, suggesting that beneficial therapeutic effects of triptolide on proteinuria might be attributed to a protective effect on podocytes.

According to the pathological process of membranous nephropathy, an effective therapy should have the following two effects, including the immunosuppression to prevent antibody production and protection on podocyte from injury

triggered by complement activation and C5b-9 formation. These two therapeutic effects will help to reduce proteinuia and block the progression of kidney disease. Immunosuppressive effect and direct podocyte protection of triptolide will result in potential treatment of membranous nephropathy. In this research, passive Heymann nephritis (PHN), an animal model of membranous nephropathy was induced in rats, which were then administrated triptolide orally to determine whether triptolide could reduce the proteinuria and improve podocyte injuries in this immune-mediated podocyte injury. Furthermore, we use an *in vitro* assembled functional terminal complement complex C5b-9 based on purified complement protein to explore the therapeutic mechanism of triptolide on C5b-9-induced podocyte damage.

RESULTS

Effect of triptolide on proteinuria

Present data showed that triptolide effectively reduced urinary protein/creatinine ratio in PHN rats (Figure 1). Rats with PHN developed heavy proteinuria and the ratio of urinary protein to creatinine was 29.3 ± 3.8. After treatment with triptolide, the ratio was significantly reduced on day 7 (12.3 ± 1.4 vs 22.5 ± 2.9, $P<0.01$), on day 14 (5.5 ± 0.7 vs 15.4 ± 1.9, $P<0.01$), on day 21 (2.1 ± 0.3 vs 9.8 ± 1.2, $P<0.01$) and on day 28 (0.9 ± 0.2 vs 5.3 ± 0.7, $P<0.01$). Pretreatment with triptolide also significantly reduced the urinary protein/creatinine ratio in PHN rats. However, there was no significant difference in the ratio between the rats with triptolide pretreatment and those with treatment.

Consistent with the marked decrease of proteinuria, plasma albumin level was increased after treatment with triptolide (Figure 2). Level of plasma albumin in PHN rats was significantly lower than that of healthy rats before treatment ($P<0.01$). After treatment with triptolide for 7 days, plasma albumin level of PHN rats was distinctly increased. On day 14, the therapeutic effect on plasma albumin was still obvious.

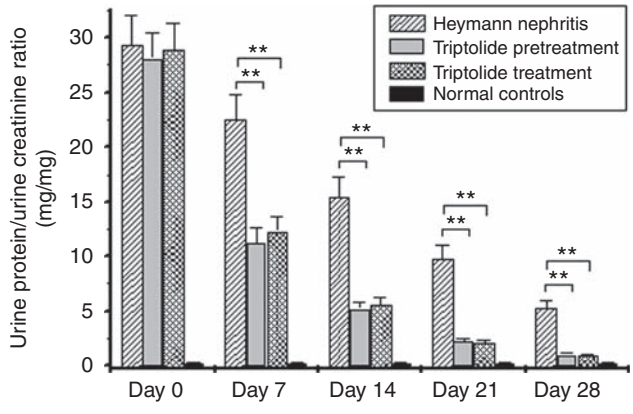

Figure 1 | Triptolide significantly reduced urinary protein/creatinine ratio in rats with passive Heymann nephritis. After treatment with triptolide for 7, 14, 21 and 28 days, the urinary protein/creatinine ratio in PHN rats was significantly reduced. There was no significant difference in the ratio between the rats with triptolide pretreatment and those with treatment. $^{**}P<0.01$ vs PHN. PHN, passive Heymann nephritis.

Effect of triptolide on glomerular histological changes

Rats with PHN showed subepithelial immune deposit formation on day 14 (Figure 3). After treatment with triptolide, subepithelial immune deposits were not significantly decreased as compared with the untreated PHN rats at the same time. Transmission electron microscopic observation indicated that there was no obvious difference in the amount of subepithelial electron dense deposits between triptolide-treated rats and PHN control rats (Figure 4).

Change of rat IgG in serum and glomeruli after treatment with triptolide

The titre of circulating rat anti-rabbit IgG antibodies in PHN rats was 100 ± 5 before treatment (10 days after the injection

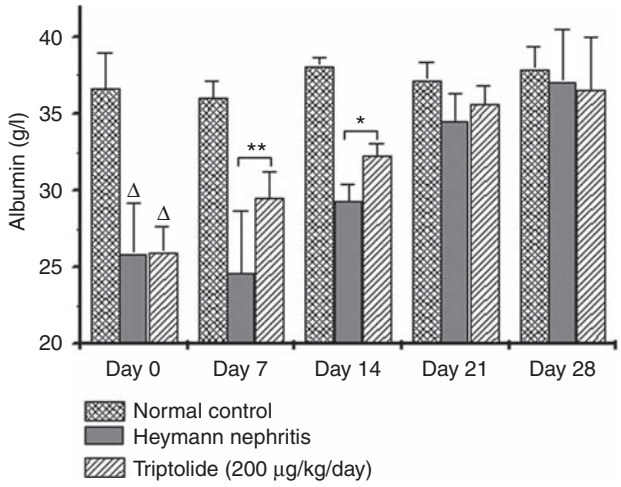

Figure 2 | Change of plasma albumin in PHN rats after treatment with triptolide. After treatment with triptolide for 7 days, plasma albumin level of PHN rats was distinctly increased. On day 14, the therapeutic effect on plasma albumin was still obvious. $^{\Delta}P>0.05$ vs PHN. $^{*}P<0.05$, $^{**}P<0.01$ vs PHN.

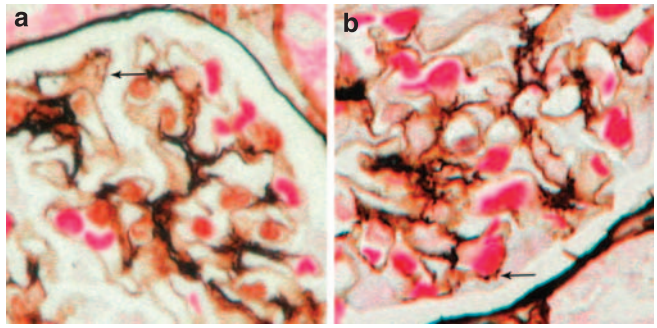

Figure 3 | Effect of triptolide on light microscopic appearance of subepithelial immune depositions of PHN rats on day 28 (PASM × 400). (**a**) PHN rats on day 28. (**b**) PHN rats treated with triptolide on day 28. Subepithelial immune depositions are shown with arrows. After treatment with triptolide, subepithelial immune deposition was not significantly decreased.

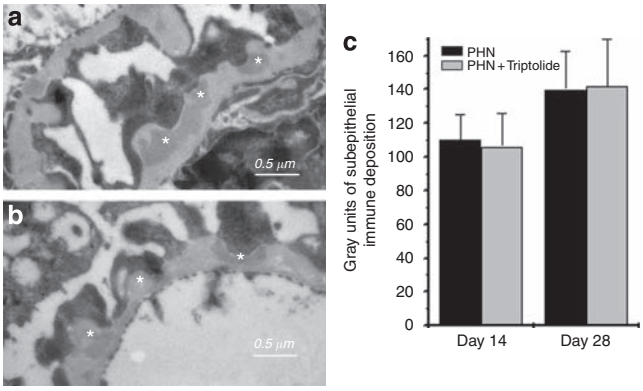

Figure 4 | Change of subepithelial immune deposition in glomeruli of PHN rats after the treatment with triptolide for 28 days (EM). (**a**) PHN rats on day 28. (**b**) PHN rats treated with triptolide on day 28. Immune deposits in the subepithelial layer are indicated by asterisks. (**c**) Semiquantification of immune deposits.

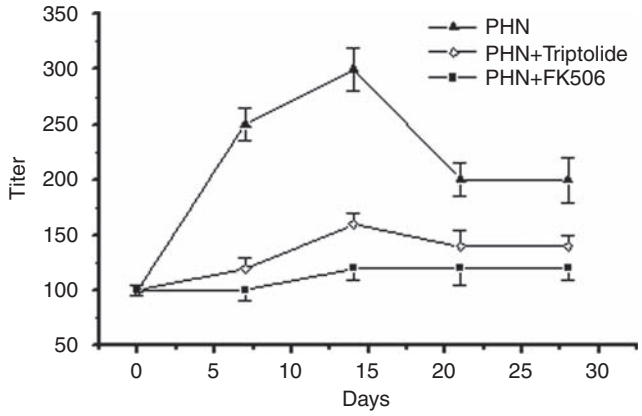

Figure 5 | Triptolide effectively reduced circulating rat anti-rabbit IgG antibodies (titer, reciprocal of the dilution) in rats with passive Heymann nephritis. $P<0.01$ vs PHN.

of anti-Fx1A rabbit serum). The titre increased to a peak of 1:(300 ± 20) on day 14 (24 days after the rabbit serum injection), then decreased gradually. After treatment with triptolide, the titre of circulating rat anti-rabbit IgG antibodies in PHN rats was markedly lower than that in PHN rats without treatment on day 7 (1:(120 ± 10) vs 1:(200 ± 15), $P<0.01$), day 14 (1:(160 ± 10) vs 1:(300 ± 20), $P<0.01$), day 21(1:(140 ± 15) vs 1:(200 ± 15), $P<0.01$), and day 28 (1:(140 ± 10) vs 1:(200 ± 20), $P<0.01$; Figure 5). After treatment with FK506, circulating rat anti-rabbit IgG antibodies in PHN rats was also effectively inhibited, the titre on day 7 was 1:(100 ± 10) and on day 14 until day 28 was 1:(120 ± 10).

Immunofluorescence staining showed that deposition of rat IgG in glomeruli of PHN rats was in granular and disperse pattern along the capillary wall. Compared with PHN rats without treatment, fluorescence intensity of rat IgG deposition decreased after treatment with triptolide for 7 and 14 days. However, on days 21 and 28, the difference in fluorescence intensity was not highly significant between PHN rats with or without triptolide treatment (Figure 6).

Change in C5b-9 deposition in the glomeruli after treatment with triptolide

Immunofluorescence staining showed that C5b-9 deposits in PHN rats had a similar pattern with IgG deposition. Compared with PHN rats without treatment, the fluorescence intensity of C5b-9 deposition decreased after treatment with triptolide for 7 and 14 days. However, on days 21 and 28 there was no significant difference on the fluorescence intensity between PHN rats with or without triptolide treatment (Figure 7).

Triptolide promoted the recovery of podocyte injuries

Desmin was used in this research as a biomarker to indicate podocyte injuries. Immunohistochemical studies showed that desmin expression was upregulated in PHN rats (Figure 8). In the normal kidney, anti-desmin antibody reacted weakly with the mesangial cells, whereas staining in the podocytes was negative. In PHN rats, conspicuously enhanced staining for desmin was noted in the podocytes, whereas triptolide treatment resulted in a decrease in desmin expression. Although desmin expression was decreased gradually in the vehicle-treated group, the desmin expression was significantly reduced in the triptolide treatment group on day 14, 21, and 28.

Results of observation with transmission electron microscopy indicated that podocyte injuries in PHN could be reversed after treatment with triptolide (Figure 9). On day 7, foot process effacement and disappearance of slit diaphragms were observed in PHN rats under the electron microscope. On days 14, 21, and 28, the injuries of podocytes, including extensive foot process effacement, were becoming more severe. After treatment with triptolide, the amelioration of podocyte injuries was remarkable. Foot process effacement was improved and reversed. Most foot processes in the triptolide-treated PHN rats were restored to a normal shape on day 28. The secondary foot process of podocytes was also restored to normal shape and structure.

Quantitative analysis of mean foot process width showed that triptolide effectively improved the reverse of foot process effacement (Figure 10). Compared with PHN rats, foot process width in the triptolide-treated group was significantly decreased on day 7 (810 ± 132 nm vs1124 ± 199 nm, $P<0.01$), day 14 (698 ± 116 nm vs1228 ± 170 nm, $P<0.01$), day 21 (584 ± 86 nm vs 827 ± 117 nm, $P<0.01$) and day 28 (508 ± 116 nm vs 732 ± 160 nm $P<0.01$). After treatment with triptolide for 28 days, the foot process width of podocytes was restored closely to the normal range.

Triptolide improved the expression and distribution of nephrin

In PHN rats, decreased expression and granular distribution of nephrin were obvious on day 7. Nephrin expression began to increase but a dot-like pattern still remained on day 14.

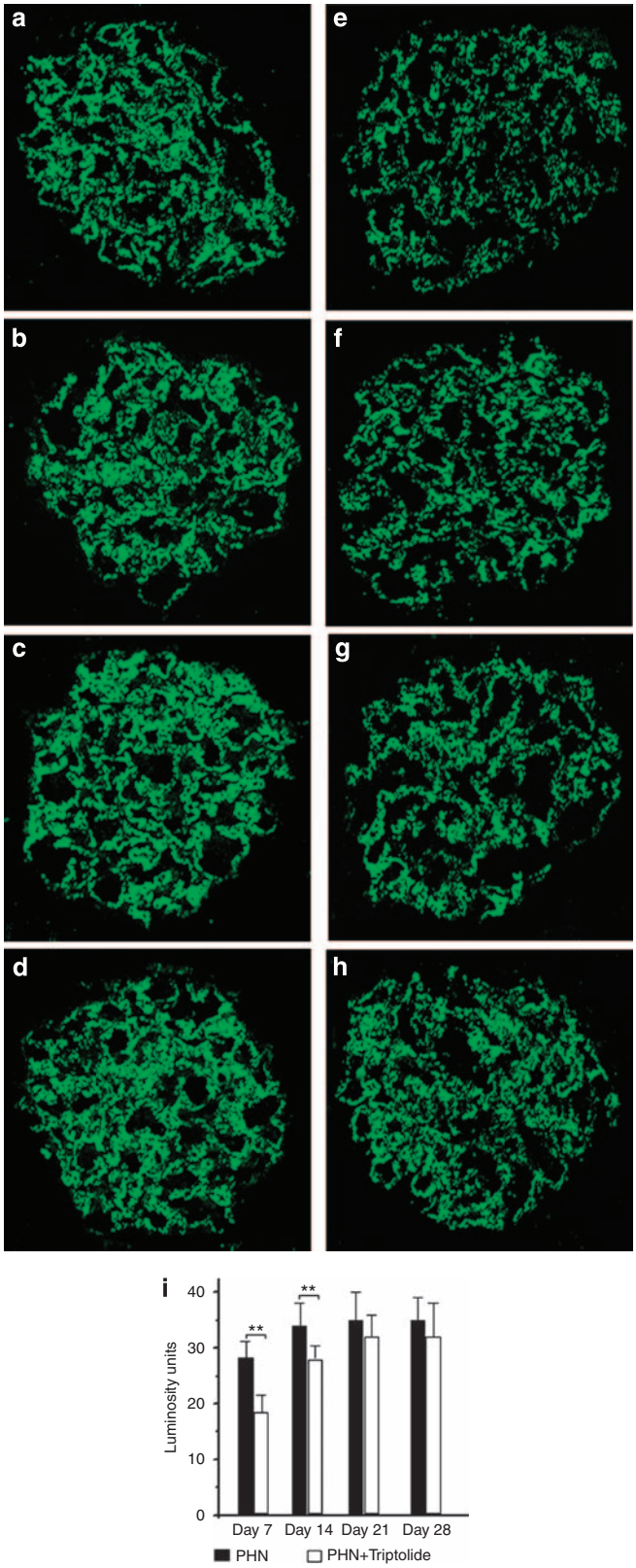

Figure 6 | The effect of triptolide on IgG deposition in glomeruli of PHN rats (magnification, × 400). (**a–d**) PHN rats on day 7, 14, 21 and 28, respectively; (**e–h**) PHN rats were treated with triptolide for 7, 14, 21 and 28 days, respectively; (**i**) quantification of the intensity of fluorescent staining for rat IgG in PHN rats after treatment with triptolide. $^{**}P<0.01$ vs PHN.

The expression and distribution of nephrin recovered gradually; however, the discontinuous pattern was still observed along the glomerular basement membrane on days 21 and 28.

Triptolide treatment significantly improved the expression and distribution of nephrin. The expression of nephrin was markedly increased after treatment with triptolide for 7 days, and the distribution pattern began to recover. The increase of expression and linear distribution of nephrin became more obvious on days 14 and 21. On day 28, both the expression and distribution of nephrin were almost completely recovered. Quantification by western blot also confirmed that triptolide remarkably improved the expression of nephrin in PHN rats (Figure 11).

Adverse effect of treatment with triptolide

Triptolide has side effects including gastrointestinal tract disturbances, leucopenia, and liver toxicities. After the induction of PHN, rats had a normal appetite and good physical condition except for proteinuria. To monitor the adverse effect of treatment with triptolide, the serum alanine transaminase (ALT), aspartate transaminase (AST), serum creatinine (Scr) and white blood cell count were examined. Oral administration of triptolide with doses used in this research had no obvious adverse effects on rats. After treatment for 28 days, ALT in the PHN groups treated with triptolide and untreated was 34.6 ± 11.0 U/l and 32.4 ± 5.41 U/l, respectively. AST in the PHN groups treated with triptolide and untreated was 91.8 ± 18.4 U/l and 83.6 ± 12.5 U/l, respectively. White blood cell count in the PHN groups treated with triptolide and untreated was $5.0 \pm 0.9 \times 10^9$/l and $4.9 \pm 0.7 \times 10^9$/l, respectively. There was no difference between the two groups treated with or without triptolide. Although serum creatinine was a little increased in the triptolide-treated group (72.6 ± 15.8 μmol/l) compared with untreated PHN rats (47.6 ± 13.6 μmol/l), the difference between two groups was not significant ($P>0.05$).

The effect of triptolide on C5b-9 assembly *in vitro*

We further used the *in vitro* assembled functional terminal complement complex C5b-9, based on purified complement protein to verify the direct effect of triptolide on C5b-9-induced podocyte injury. In these experiments, the C5b6 complex was used in limiting dilutions, while maintaining fixed concentrations of C7, C8 and C9 (10 μg/ml) to assemble C5b-9. The sublytic concentration of C5b-9 on podocytes was determined by the lactate dehydrogenase release assay. Dilutions of C5b6 <0.8 μg/ml did not increase the concentration of released lactate dehydrogenase as compared with unstimulated podocytes. However, when the concentration of C5b6 >0.8 μg/ml, significantly higher levels of lactate dehydrogenase release ($>10\%$) were noted (Figure 12A). These results showed that assembly of functional C5b-9 with the initial 0.8 μg/ml did not have a significant effect on podocyte membrane integrity. As a result, a C5b6 concentration of 0.8 μg/ml was used for subsequent experiments. The laser scan confocal microscopy assay using human

C5b-9-specific mAb aE11 showed fine granular deposits of C5b-9 on the membrane of podocytes (Figure 12C). This result was consistent with the result obtained by flow cytometry analysis. The mean fluorescence intensity of cells stained with C5b-9 antibody was apparently higher than the negative control (Figure 12B). Furthermore, the sublytic

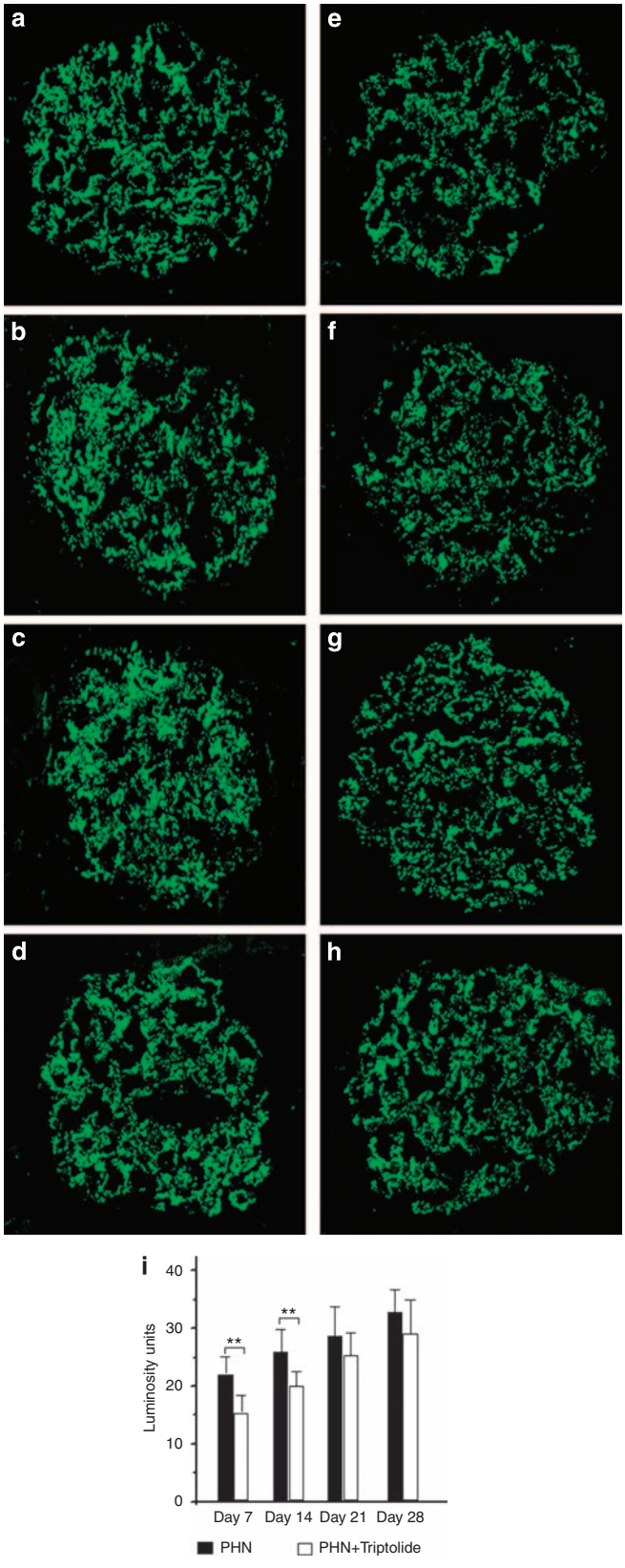

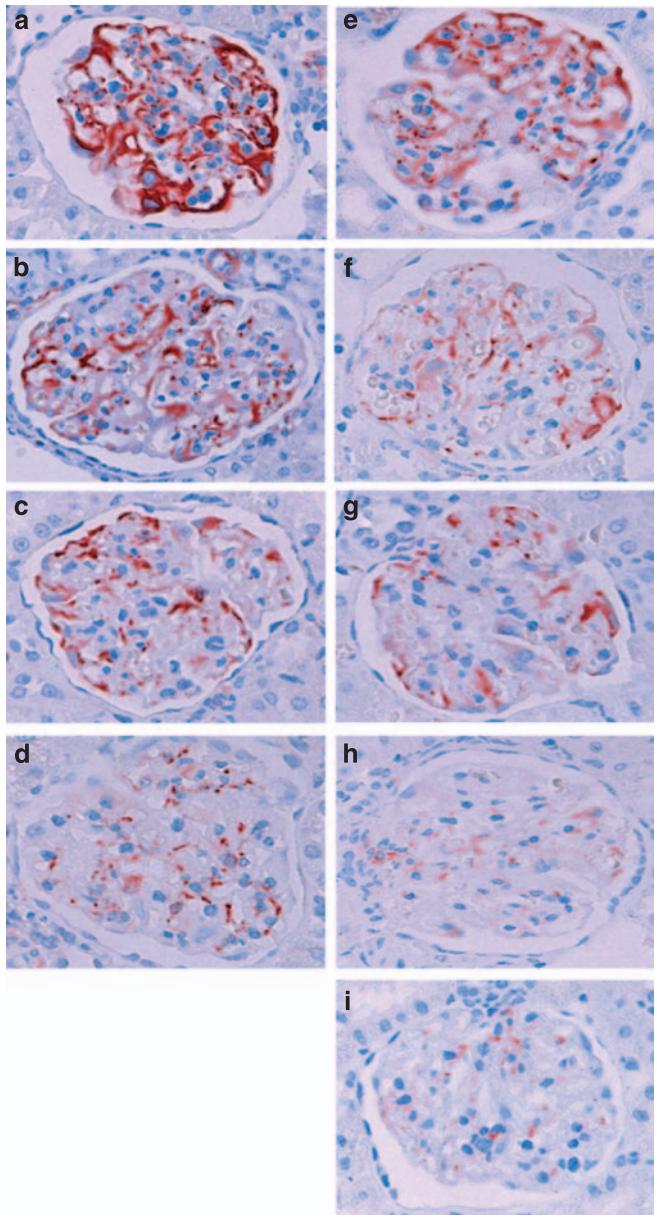

Figure 8 | The effect of triptolide on the expression of desmin, a biomarker of podocyte injuries. (**a–d**) represented the desmin expression in podocytes of PHN rats, which were treated with vehicle for 7, 14, 21, and 28 days, respectively. (**e–h**) showed that desmin expression was ameliorated after treatment with triptolide for 7, 14, 21, and 28 days, respectively. (**i**) Expression of desmin was not observed in podocytes of control rats.

Figure 7 | The effect of triptolide on C5b-9 deposition in glomeruli of PHN rats (magnification, × 400). (**a–d**) PHN rats on day 7, 14, 21, and 28 days, respectively; (**e–h**) PHN rats were treated with triptolide for 7, 14, 21, and 28 days, respectively; (**i**) Quantification of the intensity of fluorescent staining for C5b-9 in PHN rats after treatment with triptolide for 7, 14, 21, and 28 days. $^{**}P < 0.01$ vs PHN.

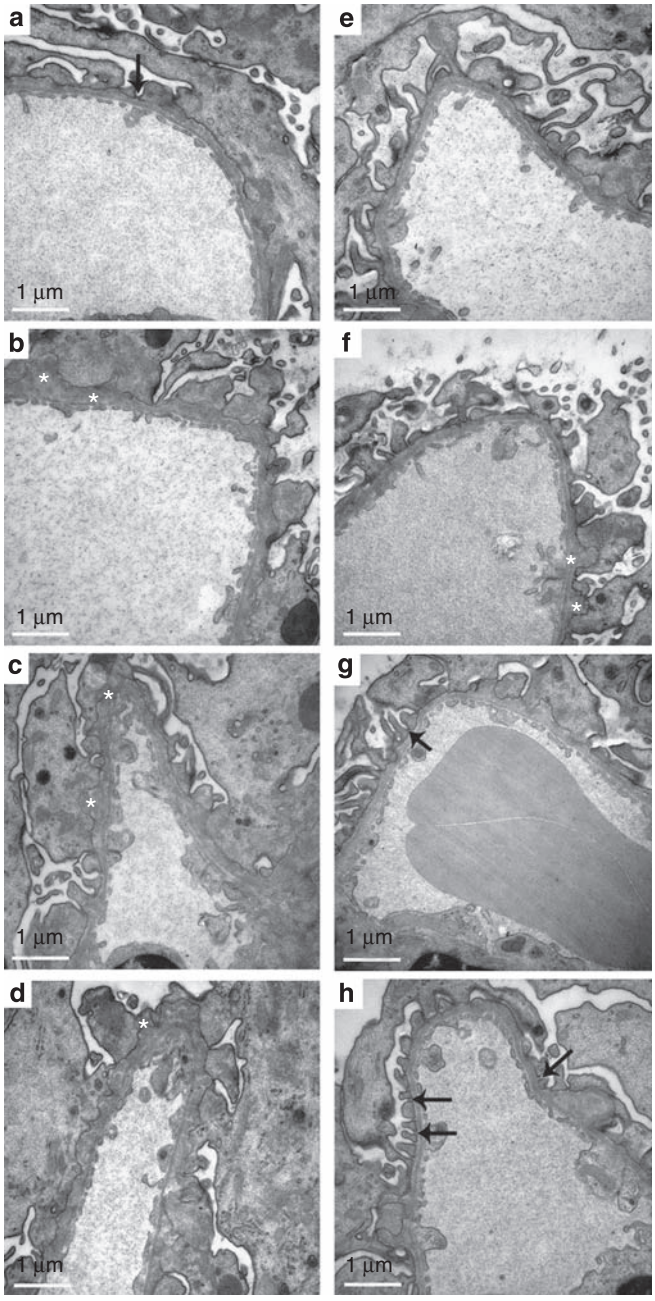

Figure 9 | Triptolide restored the foot process effacement in PHN rats. (**a**–**d**) PHN rats on day 7, 14, 21, and 28, respectively. (**e**–**h**) PHN rats were treated with triptolide for 7, 14, 21, and 28 days, respectively. Subepithelial electron-dense deposits are denoted by asterisks. Slit diaphragm is denoted by arrows. After treatment with triptolide, foot process effacement was improved and reversed. Most foot processes in the triptolide-treated PHN rats were restored to normal shape on day 28 (**h**).

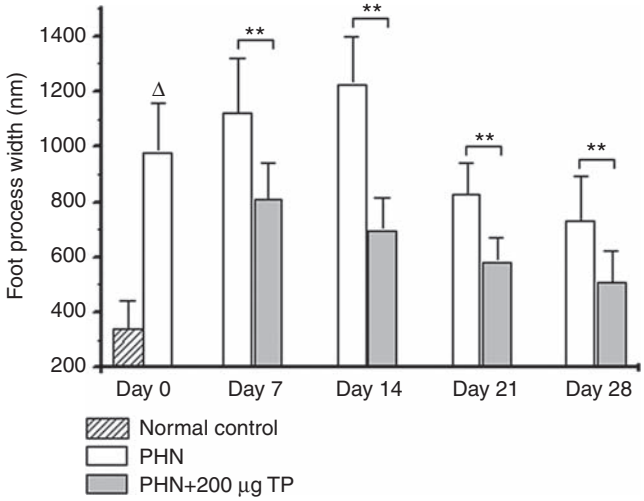

Figure 10 | Triptolide effectively reversed foot process effacement. $^{\Delta}P<0.01$ vs controls. $^{**}P<0.01$ vs PHN.

concentration of C5b-9 caused podocyte cytoskeleton reorganization in a time-dependent manner. Treatment of podocytes with C5b-9 for 30 min and 1 h only caused F-actin disorderliness and rarefaction of filaments. Treatment of podocytes with C5b-9 for 3 h resulted in dramatic loss of transcytoplasmic actin stress fiber (Figure 12D). However, disrupted actin stress fiber was partially reversed after C5b-9 treatment for 6 h.

To investigate whether the protective effect of triptolide on podocyte injury was related with the inhibition of C5b-9 assembly, we treated podocytes with triptolide for 30 min before exposure to purified complement protein and detected C5b-9 deposition on the membrane of podocytes by confocal microscopy and flow cytometry. Neither the distribution nor the intensity of the C5b-9 complex had a significant difference between the C5b-9 group and the triptolide pretreated group (Figure 13b–d). Lactate dehydrogenase release assay showed that the C5b-9-mediated cytolysis was not affected in the presence of triptolide (Figure 13a).

The effect of triptolide on cellular reactive oxygen species (ROS) production induced by C5b-9

C5b-9 increased ROS production within 30 min by nearly 4-fold compared with control in podocytes. This effect was maintained for 90 min (Figure 14A). To determine whether plasma membrane NADPH oxidase, the mitochondrial pathway, or both were responsible for intracellular ROS generation, we exposed podocytes to C5b-9 in the presence of various chemical inhibitors of these ROS synthesis pathways. Myxothiazol inhibits the mitochondrial respiratory chain at cytochrome b-c1, and TTFA is an inhibitor of mitochondria electron transport chain complex II. Mitochondrial electron chain blocker myxothiazol and TTFA had no significant effect on the increase of intracellular ROS induced by C5b-9, However, ROS production and F-actin disruption induced by C5b-9 were blocked by the NADPH oxidase inhibitor apocynin and DPI in podocytes (Figure 14B and D).

Pretreatment of podocytes with triptolide (10 ng/ml) before C5b-9 exposure led to a significant reduction in the cellular ROS level (Figure 14B). However, when podocytes were treated with triptolide (10 ng/ml) after C5b-9 had been

assembled for 30 min, it was observed that triptolide had no significant inhibitory effect on C5b-9-induced ROS production (Figure 14C).

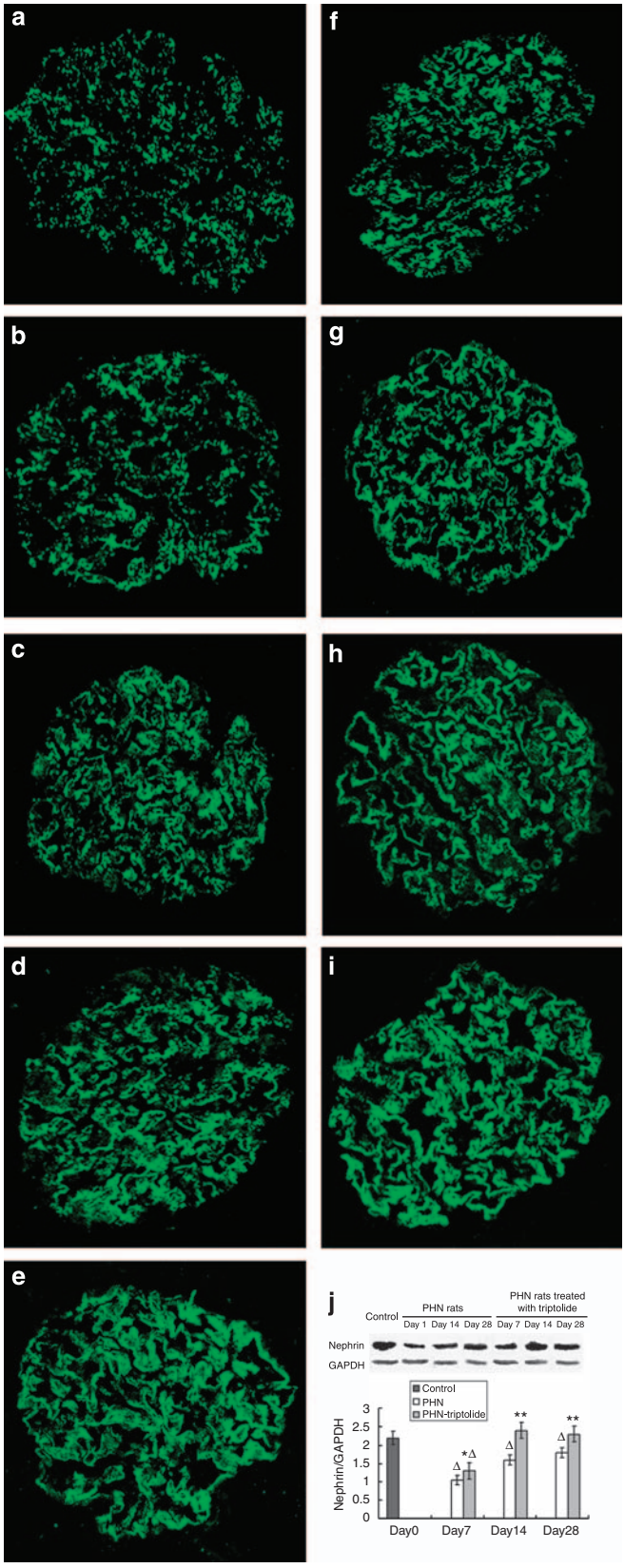

NADPH oxidase is composed of several subunits, including the $p47^{phox}$ which coalesce at the plasma membrane to form the active enzyme complex. Immunostaining confirmed the presence of the subunit $p47^{phox}$ in podocytes and showed its translocation to the plasma membrane after C5b-9 assembly. Triptolide showed inhibition of $p47^{phox}$ translocation when treated with podocytes before but not after C5b-9 assembly for 30 min (Figure 14E).

Triptolide inhibited C5b-9-induced p38 MAPK activation

To characterize the intracellular signaling pathway associated with the protective effects of triptolide in podocytes, we stimulated podocytes with C5b-9 or C5b-9 plus triptolide for various time intervals and analyzed phosphorylation of mitogen-activated protein kinases (MAPK). The family of MAPK, including p38, extracellular signal-regulated kinase (ERK) and c-Jun N-terminal kinase, is implicated in podocyte injury. C5b-9 stimulated a strong increase in phosphorylated p38 in podocytes after a 1 h incubation (Figure 15A). In contrast, C5b-9 treatment had no significant effect on phospho-ERK1/2 and phospho-c-Jun MAPK levels. The total unphosphorylated p38, ERK, and c-Jun levels were not affected. These results suggested that the activation of p38 MAPK pathway was associated with podocyte injury induced by C5b-9. Treatment of triptolide (10 ng/ml) before or after C5b-9 assembly for 30 min effectively suppressed C5b-9-induced phosphorylation of p38 MAPK (Figure 15B) in podocytes. Triptolide did not affect basal phosphorylation of p38 MAPK.

The effect of triptolide on p38 MAPK activity was also examined in PHN rats. It was found that phosphorylated p38 MAPK in the glomeruli of PHN rats was markedly decreased on day 7 and day 14 after treatment with triptolide (Figure 15D).

Activations of p38 MAPK are required for C5b-9-induced actin reorganization in podocytes

Next, we wished to determine whether increased p38 MAPK activity was required for induction of cytoskeleton disruption by sublytic C5b-9. Western blots showed that p38 inhibitor SB-203580 (5 μmol/l) significantly suppressed C5b9-induced phosphorylation of p38 MAPK, and effectively abrogated C5b-9-induced cytoskeleton disarrangement (Figure 15c3). The ERK inhibitor U0126 as well as JNK inhibitor SP600125 did not abolish C5b-9-induced cytoskeleton disruption (data not shown).

Triptolide restored the activity of RhoA in podocytes

RhoA has been suggested to have an important role in cytoskeleton reorganization. To investigate whether RhoA-signaling

Figure 11 | Triptolide significantly improved the nephrin expression and distribution on podocytes of PHN rats (magnification, × 400). (**a**–**d**) PHN rats on day 7, 14, 21, and 28, respectively; (**e**) Continuous and linear expression of nephrin in normal control; (**f**–**i**) PHN rats were treated with triptolide for 7, 14, 21, and 28 days, respectively. (**j**) Quantification of nephrin expression by western blot in PHN rats after treatment with triptolide. $^{*}P < 0.05$, $^{**}P < 0.01$ vs PHN, $^{\Delta}P < 0.01$ vs normal control.

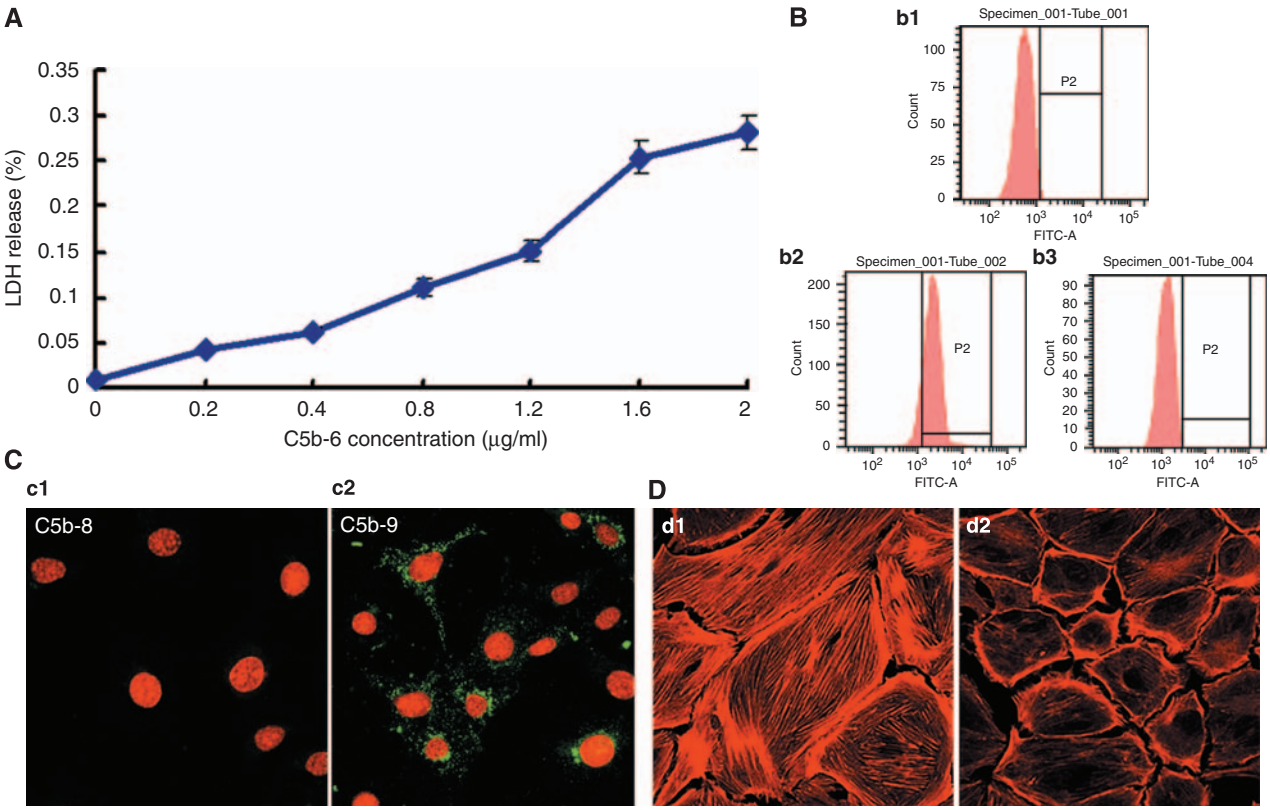

Figure 12 | Assembly of sublytic C5b-9 on podocytes with purified complement components. (**A**) Effect of C5b-9 on podocytes membrane integrity. (**B**) Flow cytometry of podocytes after C5b6–C9 assembly and incubation with mAb against C5b-9. (**b1**) Negative control (Mouse isotype antibody). (**b2**) Podocytes treated with C5b-9. (**b3**) Podocytes treated with C5b-8. (**C**) Immunofluorescence staining of podocytes with mAb against C5b-9. (**c1**) Podocytes treated with C5b-8. (**c2**) Podocytes treated with C5b-9. (**D**) C5b-9-induced actin cytoskeleton disruption. (**d1**) Untreated podocytes. (**d2**) Sublytic c5b-9-treated podocytes for 3 h. FITC, conjugated goat anti-rat IgG; LDH, lactate dehydrogenase.

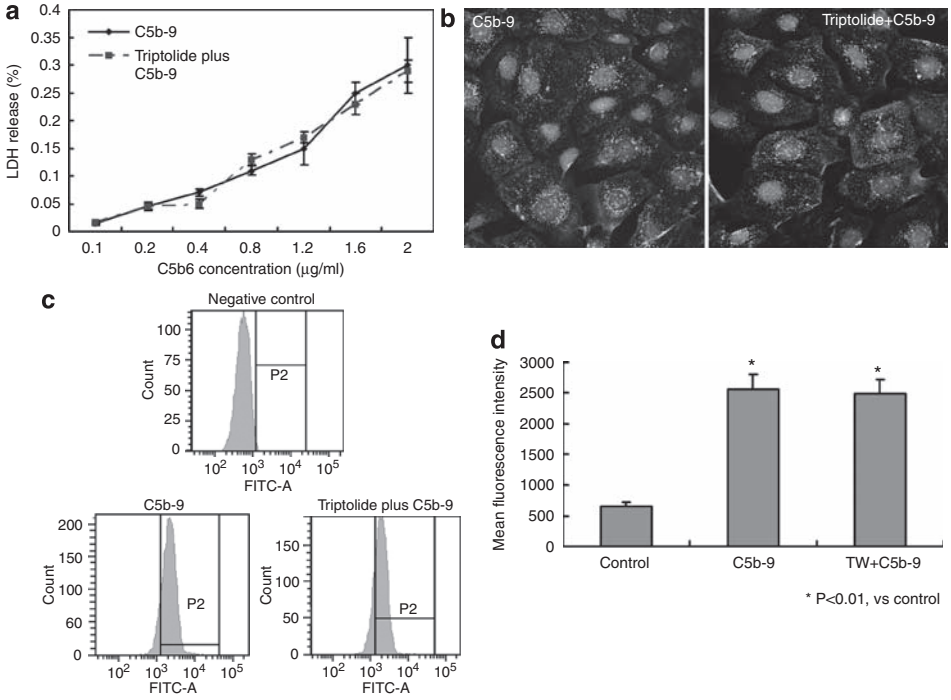

Figure 13 | The effect of triptolide on C5b-9 assembly on the membranes of podocytes. (**a**) Triptolide has no significant effect on complement-dependent cytotoxicity. (**b**) Immunofluorescence staining showed no significant difference between the C5b-9 group and triptolide-treated groups. (**c**) The amount of C5b-9 on membranes of the podocyte was detected by flow cytometry. (**d**) The C5b-9 deposits were quantified by mean fluorescence intensity ($n = 3$), *$P < 0.01$ vs negative controls.

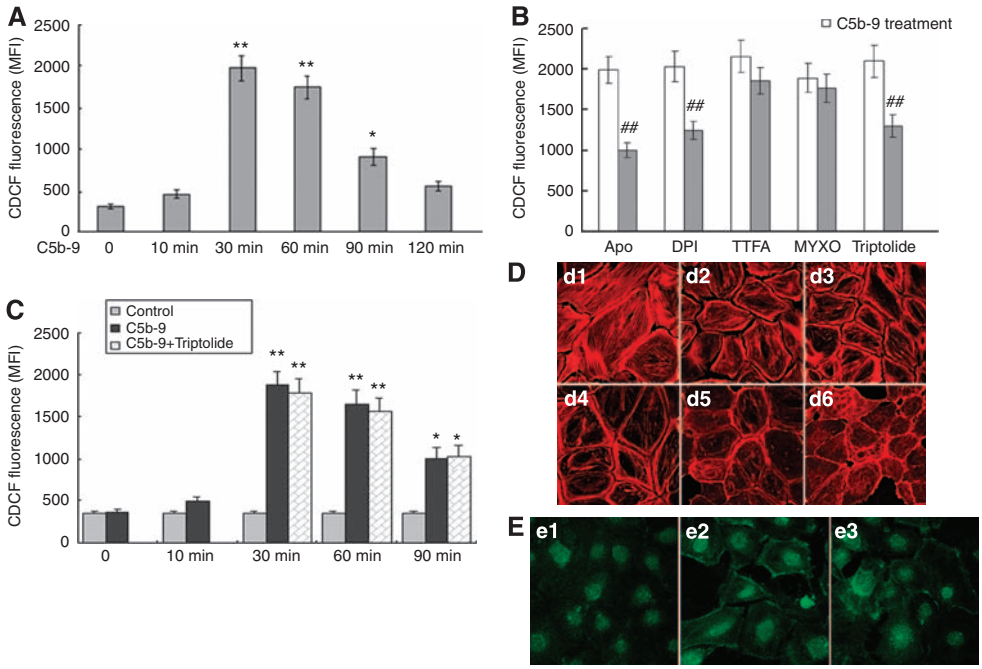

Figure 14 | Roles of the ROS generation in the protective effect of triptolide. (**A**) C5b-9-induced cellular ROS generation in a time-dependent manner. (**B**) ROS generation was examined in the presence of triptolide (10 ng/ml), NADPH oxidase inhibitors apocynin (50 μmol/l) and DPI (10 μmol/l), mitochondrial electron chain blocker TTFA (10 μmol/l) and myxothiazol (3 μmol/l). Podocytes were incubated for 30 min with the above-mentioned inhibitors before stimulation with C5b-9 for 30 min. (**C**) Triptolide has no significant inhibiting effect on C5b-9-induced ROS generation when podocytes were treated with triptolide after C5b-9 has been assembled for 30 min. (**D**) (**d1**) Normal control. F-actin disruption induced by C5b-9 prevented by triptolide (**d2**), NADPH oxidase inhibitor Apo (**d3**), and DPI (**d4**), but not mitochondrial electron chain blocker TTFA (**d5**) and myxothiazol (**d6**). (**E**) Immunostaining for the $p47^{phox}$ subunits of NADPH oxidase showed triptolide inhibited $p47^{phox}$ migration to the cellular plasma after C5b-9 treatment. (**e1**) Untreated podocytes; (**e2**) C5b-9 treated-podocytes for 30 min; (**e3**): podocytes were preincubated for 30 min with triptolide (10 ng/ml) before C5b-9 exposure. All above results presented are representative of three independent experiments. Values are expressed as mean ± s.d., $^{*}P<0.05$, $^{**}P<0.01$ vs normal control podocytes; $^{\#\#}P<0.01$ vs C5b-9-treated podocytes.

pathways are involved in the effect of triptolide on podocytes, we performed RhoA activation assay. As shown in Figure 16A and B, C5b-9 treatment induced strong decline in RhoA activity at 20 ~ 30 min. When cells were pretreated with triptolide before C5b-9 exposure, RhoA activity was partially maintained. Total protein level of RhoA was not affected by C5b-9 and triptolide treatment during the time of the test. However, the increase of RhoA activation was markedly inhibited by the specific RhoA inhibitor, C3 exoenzyme (1 μg/ml). Immunofluorescence staining was consistent with the result from western blotting, showing that inhibition of RhoA activity by C3 exoenzyme abolished the protective effect of triptolide on C5b-9-induced F-actin dissociation (Figure 16b3). These results strongly suggested that restoration of RhoA activity mediated the protective effect of triptolide.

DISCUSSION

Membranous nephropathy is one of common causes of nephritic syndrome. Central pathogenesis of membranous nephropathy is *in situ* formation of subepithelial immune deposits that produce glomerular injury by damaging and/or activating podocytes through complement-dependent processes.[13–16]

PHN, a classical rat model of human membranous nephropathy, was induced by injection into rats of rabbit antiserum against FxIA complex of the proximal convoluted tubule. As glomerular podocytes shared some antigenic determinants with the FxIA complex of the proximal convoluted tubule, rabbit antibody rapidly combine with glomerular antigen on podocytes and formed an *in situ* immune complex in the subepithelial layer of the GBM. Immune complexes can activate the complement system and result in the assembly of C5b-9 on the cell membrane. Sublytic C5b-9 could activate podocytes and induce the production of ROS and proteases by podocytes. ROS then initiated lipid peroxidation and subsequent degradation of GBM. In addition, C5b-9 formation led to cytoskeletal changes of podocytes with subsequent dissociation of nephrin from the actin cytoskeleton, resulting in foot process effacement and heavy proteinuria.[17–19] In this pathological process, the immune reaction was the initiation factor and podocyte injuries were the crucial events in the development of severe proteinuria.[19,20] Therefore, suppressing immune reaction and reducing podocyte injury become important targets in the treatment of patients with membranous nephropathy. This study showed that triptolide effectively inhibited immune response and antibody production in PHN rats, as well as reduced podocyte injury *in vitro* and *in vivo*.

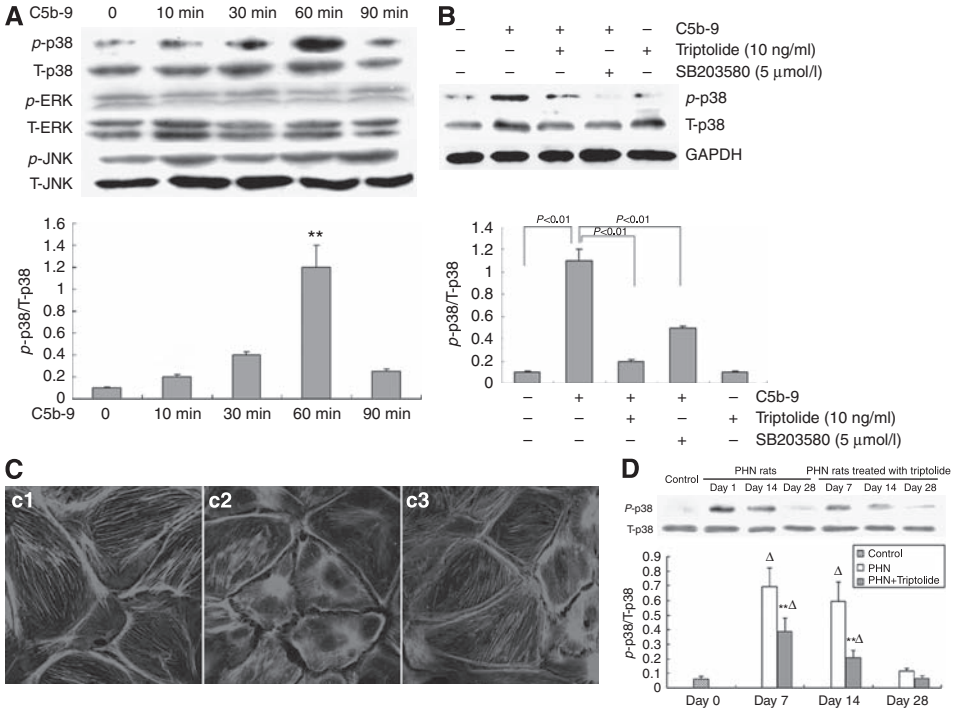

Figure 15 | Roles of p38 MAPK-signaling pathways in the protective effect of triptolide. (**A**) Time course of C5b9 on p38 MAPK activation. (**B**) Triptolide diminished p38 MAPK activation in C5b-9-treated podocytes. (**C**) p38 MAPK activation are required for C5b9-induced actin reorganization in podocytes. (**c1**) Untreated podocytes; (**c2**) C5b-9 treated podocytes for 3 h; (**c3**): podocytes were preincubated for 30 min with 5 μmol/l SB-203580 before C5b-9 exposure. All above results presented are representative of three independent experiments. Values are expressed as mean ± s.d., $^{**}P<0.01$ vs time point 0 h. (**D**) Western blotting for phosphorylated p38 MAPK in glomeruli of PHN rat treated with triptolide. $^{**}P<0.01$ vs PHN $^{\Delta}P<0.01$ vs Day 0 (control).

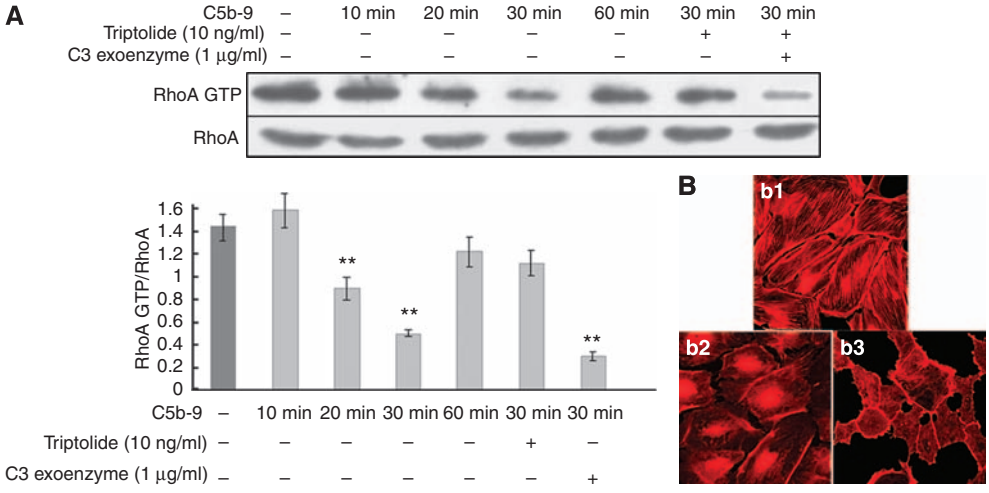

Figure 16 | Role of the RhoA-signaling pathway in the protective effect of triptolide. (**A**) Time course of RhoA activity inhibited by C5b-9 in podocytes. Triptolide restored RhoA activity in C5b-9-treated podocytes, and RhoA inhibitor C3 exoenzyme abolished the effect of triptolide. (**B**) C3 exoenzyme blocked the protective effect of triptolide on cytoskeleton in podocytes. (**b1**) Untreated podocytes; (**b2**) C5b-9-treated podocytes for 3 h; (**b3**): podocytes were preincubated for 30 min with triptolide and C3 exoenzyme before C5b-9 exposure. All the above results are representative of three independent experiments. Values are expressed as mean ± s.d.; $^{**}P<0.01$ vs untreated podocytes.

There is mounting evidence showing that triptolide has strong immunosuppressive and anti-inflammatory activities. Triptolide can not only inhibit the proliferation of lymphocytes, but also inhibit the production of many cytokines and inflammatory mediators.[8,21] In this research, triptolide was given after severe proteinuria appeared in the autologous phase. Development of PHN included the heterologous and autologous phase. During the heterologous phase, injections

of heteroantibody specific for glomerular antigens led to accumulation in the glomeruli. After 3–6 days the deposited antibody might induce transient proteinuria. In the following 3–4 days, the recipient rats usually developed an immune response to the heterologous immunoglobulin. The resulting autologous antibody bound to the heteroantibody, which was still present in the glomeruli, thereby inciting a new phase of nephritis. The autologous phase was typically more pronounced and persistent than the heterologous phase.[22,23] Therefore, we started treatment with triptolide in PHN rats 10 days after anti-Fx1A antiserum injection when proteinuria was fully established.

After treatment with triptolide, the titre of circulating rat anti-rabbit IgG antibodies in PHN rats was markedly inhibited. FK506, an immunosuppressive drug, could also effectively inhibit the circulating anti-rabbit IgG antibodies in PHN rats. The inhibition pattern was similar with triptolide although the inhibition effect was stronger than that of triptolide. These results indicated that triptolide decreased the production of circulating IgG in PHN rats through its immunosuppressive effect.

Although the glomerular deposition of IgG and C5b-9 was reduced by treatment with triptolide at the beginning of the treatment, the decrease of C5b-9 deposition is not parallel to the reduction in proteinuria. On days 21 and 28, there was no difference on the fluorescence intensity of C5b-9 between PHN rats with or without triptolide whereas proteinuria was markedly decreased in the group with tripolide treatment. Electron microscopic observation indicated that triptolide treatment could not obviously reduce the subepithelial immune deposits. Therefore, the effect of triptolide on reducing urinary protein could not be attributed to its immunosuppressive activity because immune-mediated injury happened much early in PHN rats. It was reported that rat C3 deposition became clearly positive on day 2 and significant podocyte injuries could be detected on day 7.[23,24] In this research, triptolide treatment started 10 days after the injection of rabbit anti-Fx1A antibodies. Local therapeutic effect of triptolide on podocytes might be more important.

Pretreatment with triptolide also significantly reduced the ratio of urinary protein to creatinine in PHN rats. However, there was no difference on reducing proteinuria between the triptolide treatment group and pretreatment group. In addition, there was no significant difference in the immune deposits including IgG, C3 and C5b9 between the triptolide treatment group and pretreatment (data not shown). These results indicated that non-immune effect of triptolide also has important roles in reducing urinary protein.

The direct protective effect of triptolide on podocyte injury has been confirmed by our previous studies in rats with PAN-induced nephrosis.[12] Injection of PAN in rat produces severe proteinuria as a result of PAN-injured podocytes. It was shown that pretreatment and treatment with triptolide effectively reduced the proteinuria in rats with PAN-induced nephrosis. The antiproteinuric effect was associated with improvement in the foot process effacement, a decrease in the podocyte injury marker desmin as well as the restoration of nephrin and podocin expression and distribution. In this research, pretreatment with triptolide could significantly reduce the urinary protein in PHN. The difference between the triptolide pretreatment and treatment was not significant as in the PAN-induced nephrosis. Similar observation on immune-mediated model and non-immune mediated model suggested that triptolide has direct therapeutic effects on local podocyte injuries in PHN rats.

It was reported that calcineurin inhibitors reduced proteinuria at the cost of a significantly decreased GFR. In our previous work, we confirmed that triptolide had no effect on GFR levels at the administered dose, which further proved its independent action of reducing proteinuria.[12] Taken together, we assumed that triptolide may have a direct protective effect on podocyte injury in addition to immunosuppression in this model.

An *in vitro* study further proved that triptolide could protect podocyte from PAN-induced cytoskeleton disruption, abnormalities in nephrin and podocin expression through inhibition of ROS generation and the subsequent p38 MAPK pathway, as well as restoration of RhoA activity. In PHN rats we found that signs of podocyte injury were recovered after triptolide treatment. Expression of desmin diminished after treatment with triptolide, and quantitative analysis of the mean foot process width showed that effacement of foot processes was substantially reversed. Furthermore, triptolide effectively restored the abnormalities of nephrin expression and distribution. These results showed that podocyte injuries in PHN could be reversed after treatment with triptolide.

To explore the underlying mechanism of triptolide action, an *in vitro* model of C5b-9-induced podocyte injury was used in this study. C5b-9 is crucial in the development of podocyte injuries in membranous nephropathy. C5b-9 in sublytic quantities stimulates podocytes to produce proteases, oxidants, prostanoids, extracellular matrix and cytokines. C5b-9 also causes alterations of the cytoskeleton that lead to abnormal distribution of the slit diaphragm protein. These events result in disruption of the functional integrity of the glomerular basement membrane and the protein filtration barrier of podocytes with subsequent development of massive proteinuria.[20] We assembled functional C5b-9 on the membranes of podocytes *in vitro* based on purified complement protein and observed that C5b-9 in sublytic concentration caused disruption of F-actin cytoskeleton in podocytes *in vitro*. Actin filament is a major constituent of foot processes, and depolymerization of actin filaments leads to foot process effacement.

There is accumulating evidence showing that complement attack on various cells can induce generation of ROS.[25–27] Oxidative stress induced by excess production of ROS has been implicated in pathological processes of membranous nephropathy. In support of a pathogenic role of oxidant stress in membranous nephropathy, studies that have used antioxidants and oxygen radical scavengers have shown beneficial effects in the Heymann nephritis models,[28,29] and

also in a pilot study of human membranous nephropathy.[30] Our study showed that sublytic C5b-9-induced ROS generation in podocytes was markedly increased within 30 min and this effect was maintained for 90 min. And the present results suggested that NADPH oxidase, rather than mitochondria, were the primary source of superoxide production during the C5b-9 attack. NADPH oxidase is a multicomponent enzyme comprising a plasma membrane-bound subunit, gp91; a membrane-associated flavocytochrome, cytochrome b558; and at least three cytosolic subunits, $p47^{phox}$ $p67^{phox}$ and the small G protein Rac2.[31] During activation, the $p47^{phox}$ component is phosphorylated and migrates to the plasma membrane, where it associates with the other subunits to form the active enzyme complex. Triptolide had been found to inhibit PAN-induced cellular ROS in podocytes. In this study, we found pretreatment podoyctes with tripolide lead to inhibition of $p47^{phox}$ translocation and blocked the production of ROS induced by C5b-9. However, it was observed that triptolide had no significant inhibitory effect on C5b-9-induced ROS generation when podocytes were treated with triptolide after C5b-9 has been assembled for 30 min. It may be due to the time point of tripotolide adding to the culture system. NADPH oxidase activity is transient with many stimuli.[32] Furthermore, Alder[25] showed in mesangial cell that production of H_20_2 after stimulation with membrane attack complex continued to increase during 60 min of incubation, whereas production of O_2^- after stimulation with membrane attack complex increased during the first 20 min of incubation, but then plateaued. The study of Ren[33] showed that triptolide effectively scavenged superoxide anion radical (O_2^-), but not hydroxyl radical (OH^-) as detected by electron spin resonance and spin trapping. In rats with Heymann nephritis, the fact that triptolide reverses previous podocyte injuries in the presence of C5b-9 suggests that triptolide may target downstream molecules of ROS.

ROS may damage cells through direct oxidation of lipids, proteins and DNA or it can act as a signaling molecule to trigger intracellular pathways leading to cell injury. In this study, we evaluated the effect of triptolide on the MAPK-signaling pathway as the downstream targets of cellular ROS. There are at least three MAPK pathways as follows: ERK-1/2 (p44/p42), c-Jun NH2-terminal kinase (JNK), and p38 MAPK. All three MAPK pathways may contribute to ROS-mediated cell injury.[34–36] We found that C5b-9 stimulated a strong increase in phosphorylated p38 in podocytes after 1 h of incubation. In contrast, C5b-9 treatment had no significant effect on phospho-ERK1/2 and c-jun MAPK. P38 is the major MAP kinase activated by oxidative stress in several cells under various stimuli. It is believed that activation of p38 MAPK is related to podocyte injury and development of proteinuria, as well as actin cytoskeleton disruption.[37] A study by Ren *et al.*[38] has also shown that C5b-9 assembly leads to glomerular epithelial cell injury via apoptosis signal-regulating kinase 1 and p38 in glomerular epithelial cell which overexpressed apoptosis signal-regulating kinase 1. In our study, we showed that p38 MAPK inhibitor SB-203580 successfully reduced C5b-9-induced podocyte damage, indicating that p38 MAPK phosphorylation mediated C5b-9-induced podocyte injury. In addition, we found that triptolide significantly inhibit C5b-9-induced p38 MAPK activation in podocytes. Chen *et al.*[39] showed that triptolide blocked MAP kinase phosphatase-1 expression. MAP kinase phosphatase-1s have an important role in the feedback control of MAP kinase signaling.[40] However, the concentration of triptolide (5 μmol/l) used to suppress MAP kinase phosphatase-1 expression is much higher than that used in our study. The mechanism by which triptolide regulate C5b-9-induced p38 MAPK activity needs further study.

Small GTPase-Rho-mediated signal transduction is a ubiquitous pathway in various kinds of cells. It is a direct upstream signaling that controls actin filament reorganization, directing cellular behaviors and phenotypic alterations. RhoA also has an important role in podocyte cytoskeleton organization.[41] Proper regulation of Rho GTPase is required for maintaining differentiation of podocytes.[42] We hypothesized that RhoA might also contribute to the protective effects of triptolide against C5b-9-induced lesions. We found that triptolide pretreatment restored RhoA activity, which was suppressed in C5b-9-treated podocytes. In addition, C3 exoenzyme, a highly selective inhibitor of RhoA, abolished the effect of triptolide, as shown by western blotting and immunofluorescence staining. These findings strongly suggested that restoration of RhoA activity mediated the protective effect of triptolide.

Complement regulatory proteins, such as CD59, inhibits assembly of complete large membrane attack complex within the membrane of a cell under attack.[43] However, unlike complement regulatory proteins, triptolide did not affect C5b-9 assembly, as shown by indirect immunofluorescence and confocal microscopy, as well as flow cytometry using antibody targeting poly-C9 component.

In summary, triptolide can effectively reduce proteinuria and inhibit immune-mediated injuries in PHN. This antiproteinuric effect accompanied with recovery of podocyte injuries in this model, including a decrease in desmin expression, restoration of nephrin redistribution, and foot process effacement. Multiple signal pathways involved in the effect of triptolide on podocytes. Both the immunosuppressive effects and podocyte protection contribute to the therapeutic effect of triptolide in Heymann nephritis.

MATERIALS AND METHODS

Reagents

Triptolide (C20H24O6, molecular weight 360) was obtained from Chinese National Institute for Control of Pharmaceutical and Biological Products (Beijing, China). The purity of triptolide was detected by high-performance liquid chromatography to be 99.99%. Triptolide was reconstituted in 0.01% dimethyl sulfoxide and freshly diluted with culture medium before use. Dimethyl sulfoxide's concentration in *in vitro* studies was less than 0.002% (v/v). FK506 was provided by Fujisawa Pharmaceutical Co. and dissolved in saline. Purified complement components including C5b6, C7, C8 and C9 were purchased from Calbiochem (San Diego, CA, USA).

Apocynin, 2-thenoyltrifluoroacetone (TTFA), myxothiazol, and diphenyl iodonium (DPI) were purchased from Sigma (St Louis, MO, USA).

Induction of passive Heymann nephritits

FxIA tubular antigen was prepared from renal cortices of Wistar rats. New Zealand white rabbits were immunized with FxIA antigen and the rabbit antiserum was prepared. Adult female Sprague–Dawley (SD) rats (Experimental Animal Center, Jinling Hospital, Nanjing) with body weights of 150 to 180 grams were given two intraperitoneal injections of anti-Fx1A antiserum, 2 and 1 ml sequentially with 1 hour intermission. 24-h urine collections were done on individual rats in metabolic cages. Protein content was determined by the Bradford method. Urine creatinine was detected by enzymatic method with kits (Randox, Crumlin, County Antrim, North Ireland). Treatment with triptolide started 10 days after antiserum injection when proteinuria was already present.

Rats with passive Heymann nephritis ($n=32$) were orally administered triptolide (200 μg/kg/d). For the pretreatment group, rats ($n=6$) were pretreated with triptolide (200 μg/kg/d) 2 days before the induction of PHN and continued throughout the experiment. In the treatment group with FK506, rats ($n=6$) were orally administered 1 mg/kg of FK506. As controls, another 32 rats with passive Heymann nephritis were given an oral dose of 1 ml normal saline solution containing 0.4% dimethyl sulfoxide every day. 10 healthy rats were chosen as normal controls.

Schedule of laboratory tests and sample collection

Rats were housed under standard conditions (air-conditioned room, 22°C) with free access to food and water. After proteinuria was established in PHN rats, treatment with triptolide started on day 1 and continued until day 28. Once a week, 24-h urine samples were collected after the rats had been transferred to metabolic cages with free access to water but without food. After treatment with triptolide for 7, 14, 21 and 28 days, blood samples were taken from the retro bulbar plexus of the ketamine-anesthetized rats, eight rats in each group were killed after ketamine narcosis. Blood and urine samples were immediately subjected to standard laboratory tests to measure serum levels of albumin, aminotransferases, creatinine, and white blood cell count. Renal tissues were processed for morphological studies and immunofluorescence microscopy.

Assay of circulating rat antibodies against rabbit

The amount of circulating antibodies to rabbit IgG was determined using ELISA. Plates (Organon Teknika, Ireland) were coated with 4.0 μg/ml rabbit IgG in 0.1 M sodium carbonate buffer (pH 9.6) and incubated for 20 h at 4°C. After blocking with 1% BSA and then washing the plates with PBST (10 mM PBS, pH 7.4, 0.2% Tween 20), rat serum of PHN rats with or without treatment with triptolide were added and incubated for 1 hour at 37°C. After washing with PBST, Horseradish peroxidase (HRP) labeled sheep polyclonal antibody against rat (1:2000, Southern Biotechnology Associates, Birmingham, AL, USA) was applied and incubated for 1 hour. After washing, o-phenylenediamine and H_2O_2 were added. The reaction was terminated by 1 M H_2SO_4. The absorbance was measured chromatically at 492 nm with an ELISA-reader (Thermo Multiskan Spectrum, Waltham, MA, USA).

Morphological studies by light microscopy

Kidney tissues were fixed in 10% formalin, dehydrated in graded alcohol and embedded in paraffin. 2 μm sections were cut and stained with hematoxylin and eosin, periodic acid-Schiff regent, periodic acid-sliver methenamine and Masson's trichrome. All slides were evaluated by the same pathologist who was unaware of the nature of the experimental groups at Nikon E800 microscope.

Morphological studies by transmission electron microscopy

Blocks of renal cortex tissue (1 mm^3) were fixed in cold 3.75% glutaraldehyde for 4 h. After washing in 0.1 M phosphate buffer (pH 7.5) for 5–6 times, renal tissue was post fixed in 2% osmium tetroxide for 2 h, dehydrated in graded acetone and ethanol, and embedded in epoxy resin (SPI, Indianapolis, IN, USA). Ultra thin sections (80–90 nm) were stained with uranyl acetate and lead citrate, then examined and photographed in a Hitachi 7500 transmission electron microscope (Hitachi, Tokyo, Japan).

For evaluation of the foot process width per length of GBM, images covering one glomerular cross-section were obtained in electron microscope. With the use of SimplePCI software (Compix, Irvine, CA, USA), the length of the peripheral GBM was measured and the number of foot process overlying this GBM length was counted. The arithmetic mean of the foot process width was calculated as : $(\pi/4) \times (\sum \text{GBM length}/\sum \text{number of foot process})$,[44] where $\sum$GBM length is the total GBM length measured in one glomerulus, $\sum$number of foot process is the total number of foot process counted. The correction factor $\pi/4$ serves to correct the random orientation in which the foot processes are sectioned.

For semiquantification of the subepithelial immune deposits, all exposure settings were kept constant for each group of kidneys. Subepithelial dense deposits around each capillary were outlined and the gray value of subepithelial immune deposits was read from the Histogram command in Adobe Photoshop.[24]

Immunofluorescence and immunohistochemistry

Renal cortex was embedded in Tissue-Tek OCT Compound, snap-frozen in liquid nitrogen and cut in a cryostat (Leica CM 3050S, Nussloch, Germany).

To observe the deposition of IgG and C5b-9 in glomeruli, 4 μm cryosections were fixed in acetone, washed with cold PBS, blocked with 1% bovine serum albumin in PBS, and stained with fluorescein isothiocyanate (FITC)-conjugated goat anti-rat IgG(1:100, Chemicon, Billerica, MA, USA), mouse anti-rat C5b-9(1:100, DAKO, Carpinteria, CA, USA), which was followed by FITC-conjugated goat anti-mouse IgG(1:50, DAKO).

To observe the expression and distribution of nephrin, the sections were stained with mouse anti-rat nephrin, mAb 5-1-6 (1:400, a gift from professor Hiroshi Kawachi in Niigata University, Japan), followed by FITC-conjugated goat anti-mouse IgG(1:50, DAKO). All the sections were examined by immunofluorescence microscope (Nikon Eclipse E800, Tokyo, Japan). All exposure settings were kept constant for each section.

The sections were examined by epifluorescent microscopy that used a Nikon Pan Fluor lens. The images were captured with a Spot CCD camera and exported into Adobe Photoshop. All exposure settings were kept constant for each group of kidneys. Fluorescence intensity was measured by outlining the perimeter of six glomeruli in each section and reading the luminosity from the Histogram command in Adobe Photoshop.[44] Calibration of the CCD exposure time assured that the settings chosen were in the linear range and well below saturation.

For immunohistochemical analysis of desmin expression, sections were incubated with mouse monoclonal antibody against rat desmin (D33, DAKO) for 1 h. Then the sections were incubated

with HRP-conjugated secondary antibody (Envision kit, DAKO) for 40 min. Color was developed by incubation with AEC (DAKO) and the sections were counterstained with hematoxyline. All the sections were examined by a microscope (Nikon E800) and all exposure settings were kept constant for each section.

Mouse podocyte culture

Conditionally immortalized mouse podocytes were a kind gift from Professor Stuart J Shankland (University of Washington, Seattle, WA, USA). Podocytes were cultured in RPMI-1640 medium containing 10% fetal bovine serum, 100 U/ml penicillin, and 100 mg/ml streptomycin (Gibco-BRL, Gaithersburg, MD, USA). Podocytes were expanded by culture in a medium containing 10 U/ml mouse interferon-γ (R&D Systems, Minneapolis, MN, USA) at 33°C. Removal of interferon-γ and switching growth temperature to 37°C for 10–14 days caused podocytes to stop proliferating and undertake a differentiated phenotype.[45] Podocytes were starved from FCS for 24 h before all experiments.

Assembly of C5b-9 membrane attack complex on podocytes *in vitro*

Purified human complement components C5b-6 to C9 were used to assemble C5b-9. The capacity of this complex to lyse chicken erythrocytes was confirmed before use. Differentiated podocytes were washed three times with serum-free medium. Assembly of intact C5b-9 was initiated by a 15 min pre-incubation (37°C) with C5b-6 (0.8 μg/ml) and C7 (10 μg/ml), then complement component C8 and C9 (10 μg/ml each) were added, and cells were incubated for an additional 30 min.[46] Podocytes were washed with serum-free medium to remove excess non-complex complement components and incubated with serum-free medium for indicated time. Alterations of membrane integrity because of the formation of C5b-9 complex were determined by measuring the release of enzyme lactate dehydrogenase (LDH) using a kit purchased from Roche (No. 1644793; Grenzach-Wyhlen, Germany). The formation of C5b-9 on the membrane of podocytes were verified by confocal microscopy (LSM 510, Carl Zeiss, Jena, Germany) and flow cytometry (FACS Aria, Becton Dickinson, San Jose, CA, USA) using antibody to C5b-9 (DAKO). In experiment with triptolide acting on C5b-9 assembly, podocytes were pretreated with triptolide (10 ng/ml) for 30 min before adding C5b-9.

Actin cytoskeleton staining and $p47^{phox}$ immunostaining

Cells were fixed with 4% paraformaldehyde, incubated with 0.5% Triton X-100 for 10 min, and stained with 0.5 ng/ml Rhodamin–phalloidin (Cytoskeleton, Denver, CO, USA) for 40 min in darkness. Subcellular localization of the $p47^{phox}$ subunits of NADPH oxidase was evaluated in podocytes fixed with 4% paraformaldehyde for 20 min on ice. After preincubation in blocking buffer, the cells were incubated with a 1:50 dilution of goat anti-$p47^{phox}$ (Santa Cruz Biotechnology, Santa Cruz, CA, USA). After washing, the cells were incubated with 1:50 dilutions of FITC-conjugated donkey anti-goat IgG (Santa Cruz). Negative controls were prepared by omitting the primary antibodies. Cover glasses were mounted, and the slides were examined by immunofluorescence microscope (Nikon Eclipse E800).

Reactive oxygen species (ROS) assay

The intracellular production of ROS was assayed using the fluoroprobe CM-H_2DCFDA (chloromethyl-2, 7-dichlorodihydro-fluorescein diacetate, Molecular Probes, Eugene, OR, USA). To examine the effect of C5b-9 on ROS generation by podocytes, podocytes were stimulated with C5b-9 for 10, 30, 60 and 90 min. To determine the effect of triptolide on C5b-9-stimulated ROS generation, podocytes were treated with triptolide (10 ng/ml) before or after C5b-9 has been assembled for 30 min, After the treatment, cells were loaded with 10 ìmol/l CM-H_2DCFDA. Cells were immediately analyzed using flow cytometry. For each sample, 10,000 events were collected and the content of ROS was assessed by mean fluorescence intensity (MFI).

Western blot analysis of MAPK activation

Glomeruli of experimental rats were isolated by the standard sieving method. The glomeruli or cultured podocytes were rinsed with ice cold PBS with sodium orthovanadate and lysed with lysis buffer (50 mM Tris, 150 mM NaCl, 10 mM ethylenediaminetetraacetic acid, 1% Triton X-100) containing protease and phosphatase inhibitors on ice. The lysates (50 μg) were heated for 5 min at 95°C in sample buffer, separated on 10% polyacrylamide sodium dodecyl sulfate gel and transferred onto PVDF membrane. Membranes were blocked for 1 h at room temperature with 5% powdered milk in Tris-HCl buffer containing Tween 20 (TTBS). Primary antibodies were diluted in TTBS and added as follows: anti JNK and anti-phospho-JNK, anti ERK 1/2, anti-phospho-ERK1/2, anti p38, antiphospho-p38 and anti GAPDH (Santa Cruz Biotechnology; mouse monoclonal IgG, dilution 1:200); anti GAPDH (Sigma-Aldrich; mouse monoclonal, dilution 1:10,000). The membranes were incubated with primary antibodies overnight at 4°C followed by incubation with secondary antibodies (donkey anti-mouse IgG HRP-conjugated, Jackson ImmunoResearch Laboratories, West Grove, PA, USA; dilution 1:10,000) at room temperature for 1 h. Blots were detected using an enhanced chemiluminescence detection system (Millipore Corporation, Billerica, MA, USA) according to the manufacturer's instructions. Exposures were recorded on Hyper-film (Amersham Bioscience UK Ltd, Buckinghamshire, England) for different time points and quantified by use of a densitometer (Bio-Rad Laboratories, Munich, Germany).

RhoA activation assay by pull-down experiment

RhoA activation was studied using the RhoA activation kit (Cytoskeleton) according to the manufacturer's recommendations. After cell lysis, about 300 μg of protein was incubated with 50 mg of Rhotekin-RBD protein beads (GST fusion protein containing the RhoA-binding domain of Rhotekin). The bound proteins were fractionated on 12% SDS-polyacrylamide gel electrophoresis and immunoblotted with anti-RhoA monoclonal antibody. The level of active RhoA was determined after normalization with the total RhoA presented in the cell lysates.

Statistical analysis

Statistical analyses were performed with SPSS software (version 11.5). Results were expressed as mean ± s.d. Student's *t*-test was used to compare differences between groups. $P<0.05$ was considered statistically significant, and $P<0.01$ was considered highly statistically significant.

DISCLOSURE

All the authors declared no competing interests.

ACKNOWLEDGMENTS

This study was supported by the Foundations of Medical Research in China (06G040, 06Z35, 08Z025, and BKZ007718). We thank Professor David J Salant at Boston University, USA for his kind review of this paper.

We thank Professor Hiroshi Kawachi at Niigata University, Japan for providing mouse anti-rat nephrin antibody. Conditionally immortalized mouse podocytes were kindly provided by Professor Stuart J Shankland at University of Washington, USA.

REFERENCES

1. Li LS, Liu ZH. Epidemiologic data of renal diseases from a single unit in China: analysis based on 13,519 renal biopsies. *Kidney Int* 2004; **66**: 920–923.
2. Cattran DC. Idiopathic membranous glomerulonephritis. *Kidney Int* 2001; **59**: 1983–1994.
3. Cattran DC. Management of membranous nephropathy: when and what for treatment. *J Am Soc Nephrol* 2005; **16**: 1188–1194.
4. Ly J, Alexander M, Quaggin SE. A podocentric view of nephrology. *Curr Opin Nephrol Hypertens* 2004; **13**: 299–305.
5. de Zoysa JR, Topham PS. Podocyte biology in human disease. *Nephrology* 2005; **10**: 362–367.
6. Blume C, Heise G, Hess A *et al.* Different effect of cyclosporine A and mycophenolate mofetil on passive Heymann nephritis in the rat. *Nephron Exp Nephrol* 2005; **100**: e104–e112.
7. Kupchan SM, Court WA, Dailey Jr RG *et al.* Triptolide and tripdiolide, novel antileukemic diterpenoid triepoxides from Tripterygium wilfordii. *J Am Chem Soc* 1972; **94**: 7194–7195.
8. Qiu D, Zhao G, Aoki Y *et al.* Immunosuppressant PG490 (triptolide) inhibits T cell interleukin-2 expression at the level of purine-box nuclear factor of activated T cells and NF kappaB transcriptional activation. *J Biol Chem* 1999; **274**: 13443–13450.
9. Liu Q, Chen T, Chen H *et al.* Triptolide (PG-490) induces apoptosis of dendritic cells through sequential p38 MAP kinase phosphorylation and caspase 3 activation. *Biochem Biophys Res Commun* 2004; **319**: 980–986.
10. Qiu D, Kao PN. Immunosuppressive and anti-inflammatory mechanisms of triptolide, the principal active diterpenoid from the Chinese medicinal herb Tripterygium wilfordii Hook. f. *Drugs RD* 2003; **4**: 1–18.
11. Sharma M, Li JZ, Sharma R *et al.* Inhibitory effect of Tripterygium wilfordii multiglycoside on increased glomerular albumin permeability *in vitro*. *Nephrol Dial Transplant* 1997; **12**: 2064–2068.
12. Zheng CX, Chen ZH, Zeng CH *et al.* Triptolide protects podocytes from puromycin aminonucleoside induced injury *in vivo* and *in vitro*. *Kidney Int* 2008; **74**: 596–612.
13. Couser WG, Baker PJ, Adler S. Complement and the direct mediation of immune glomerular injury. *Kidney Int* 1985; **28**: 879–900.
14. Couser WG, Pruchno CJ, Schulze M. The role of C5b-9 in experimental membranous nephropathy. *Nephrol Dial Transplant* 1992; **7**(Suppl 1): 25–31.
15. Ponticelli C. Membranous nephropathy. *J Nephrol* 2007; **20**: 268–287.
16. Couser WG, Nangaku M. Cellular and molecular biology of membranous nephropathy. *J Nephrol* 2006; **19**: 699–705.
17. Saran AM, Yuan H, Takeuchi E *et al.* Complement mediates nephrin redistribution and actin dissociation in experimental membranous nephropathy. *Kidney Int* 2003; **64**: 2072–2078.
18. Ronco P, Debiec H. Molecular pathomechanisms of membranous nephropathy: from Heymann nephritis to alloimmunization. *J Am Soc Nephrol* 2005; **16**: 1205–1213.
19. Cybulsky A, Quigg R, Salant D. Experimental membranous nephropathy redux. *Am J Physiol Renal Physiol* 2005; **289**: F660–F671.
20. Nangaku M, Shankland SJ, Couser WG. Cellular response to injury in membranous nephropathy. *J Am Soc Nephrol* 2005; **16**: 1195–1204.
21. Yang Y, Liu Z, Tolosa E *et al.* Triptolide induces apoptotic death of T lymphocyte. *Immunopharmacology* 1998; **40**: 139–149.
22. Zanetti M, Druet P. Passive Heymann's nephritis as a model of immune glomerulonephritis mediated by antihodies to immunoglobulins. *Clin Exp Immunol* 1980; **41**: 189–195.
23. Salant DJ, Darby C, Couser WG. Experimental membranous glomerulonephritis in rats. *J Clin Invest* 1980; **66**: 71–81.
24. Yuan H, Takeuchi E, Taylor GA *et al.* Nephrin dissociates from actin, and its expression is reduced in early experimental membranous nephropathy. *J Am Soc Nephrol* 2002; **13**: 946–956.
25. Adler S, Baker PJ, Johnson RJ *et al.* Complement membrane attack complex stimulates production of reactive oxygen metabolites by cultured rat mesangial cells. *J Clin Invest* 1986; **77**: 762–767.
26. Hansch GM, Seitz M, Betz M. Effects of the late complement components C5b-9 on human monocytes: release of prostanoids, oxygen radicals and of a factor inducing cell proliferation. *Int Arch Allergy Appl Immunol* 1987; **82**: 317–320.
27. Shah SV. Evidence suggesting a role for hydroxyl radical in passive Heymann nephritis in rats. *Am J Physiol* 1988; **254**(Part 2): F337–F344.
28. Lotan D, Kaplan BS, Fong JS *et al.* Reduction of protein excretion by dimethyl sulfoxide in rats with passive Heymann nephritis. *Kidney Int* 1984; **25**: 778–788.
29. Kaplan BS, Milner LS, Lotan D *et al.* Interactions of dimethyl sulfoxide and nonsteroidal anti-inflammatory agents in passive Heymann's nephritis. *J Lab Clin Med* 1986; **107**: 425–430.
30. Haas M, Mayer G, Wirnsberger G *et al.* Antioxidant treatment of therapy-resistant idiopathic membranous nephropathy with probucol: A pilot study. *Wien Klin Wochenschr* 2002; **114**: 143–147.
31. Groemping Y, Rittinger K. Activation and assembly of the NADPH oxidase: a structural perspective. *Biochem J* 2005; **386**: 401–416.
32. DeCoursey TE, Ligeti E. Regulation and termination of NADPH oxidase activity. *Cell Mol Life Sci* 2005; **62**: 2173–2193.
33. Ren J, Liu P, Zhao B *et al.* Scavenging effects of Tripterygium wilfordii on oxygen free radical. *Tongji Yike Daxue Xuebao* 1997; **26**: 112–115.
34. Susztak K, Raff AC, Schiffer M *et al.* Glucose-induced reactive oxygen species cause apoptosis of podocytes and podocyte depletion at the onset of diabetic nephropathy. *Diabetes* 2006; **55**: 225–233.
35. Liu WH, Cheng YC, Chang LS. ROS-mediated p38alpha MAPK activation and ERK inactivation responsible for upregulation of Fas and FasL and autocrine Fas-mediated cell death in Taiwan cobra phospholipase A(2)-treated U937 cells. *J Cell Physiol* 2009; **219**: 642–651.
36. Benhar M, Dalyot I, Engelberg D *et al.* Enhanced ROS production in oncogenically transformed cells potentiates c-Jun N-terminal kinase and p38 mitogen-activated protein kinase activation and sensitization to genotoxic stress. *Mol Cell Biol* 2001; **21**: 6913–6926.
37. Sawai K, Mukoyama M, Mori K *et al.* Role of p38 mitogen-activated protein kinase activation in podocyte injury and proteinuria in experimental nephrotic syndrome. *J Am Soc Nephrol* 2005; **16**: 2690–2701.
38. Ren G, Huynh C, Bijian K *et al.* Role of apoptosis signal-regulating kinase 1 in complement-mediated glomerular epithelial cell injury. *Mol Immunol* 2008; **45**: 2236–2246.
39. Chen P, Li J, Barnes J *et al.* Restraint of proinflammatory cytokine biosynthesis by mitogen-activated protein kinase phosphatase-1 in lipopolysaccharide-stimulated macrophages. *J immunol* 2002; **169**: 6408–6416.
40. Keyse SM. Protein phosphatases and the regulation of mitogen-activated protein kinase signalling. *Curr Opin Cell Biol* 2000; **12**: 186–191.
41. Zhang H, Cybulsky AV, Aoudjit L *et al.* Role of Rho-GTPases in complement-mediated glomerular epithelial cell injury. *Am J Physiol Renal Physiol* 2007; **293**: F148–F156.
42. Asanuma K, Yanagida-Asanuma E, Faul C *et al.* Synaptopodin orchestrates actin organization and cell motility via regulation of RhoA signaling. *Nat Cell Biol* 2006; **8**: 485–491.
43. Farkas I, Baranyi L, Ishikawa Y *et al.* CD59 blocks not only the insertion of C9 into MAC but inhibits ion channel formation by homologous C5b-8 as well as C5b-9. *J Physiol* 2002; **539**: 537–545.
44. White KE, Bilous RW. Estimation of podocyte number: A comparison of methods. *Kidney Int* 2004; **66**: 663–667.
45. Mundel P, Reiser J, Zúñiga Mejía Borja A *et al.* Rearrangements of the cytoskeleton and cell contacts induce process formation during differentiation of conditionally immortalized mouse podocyte cell lines. *Exp Cell Res* 1997; **236**: 248–258.
46. Chen Y, Yang C, Jin N *et al.* Terminal complement complex C5b-9-treated human monocyte-derived dendritic cells undergo maturation and induce Th1 polarization. *Eur J Immunol* 2007; **37**: 167–176.